Supporting Information

Description of standard MD simulations run with parm99

In the MD_Hm_99 simulation, opening of the major groove was clearly seen after ~30 ns (Figure 4B). The major groove width increased from the original X-ray value of 8 Å up to ~17 Å and it fluctuated around this value during the rest of the simulation (Figure 4). Both sheared and rH pairs exhibited opening events (Table 2). At 150 ns, the sheared pair was disrupted and the A and G bases stacked, resulting in disruption of the adjacent Watson-Crick paired segment (residues 7-12) (Figure 1). No improvement was observed in 250 ns of additional simulation; therefore the 150-250 ns time period was not considered in the analysis. The A5A14 cross-strand stack was relatively stable, while the intrastrand stack showed dynamics (Figure 5). In particular, the original A5A6 X-ray intrastrand stack changed into an A5G13 stack after 40 ns of simulation (Figure 5).

The MD_Dr_99 simulation showed considerable widening of the major groove already during the first 10 ns (Figure 4B). The groove width increased to ~19 Å and fluctuated around this value for the rest of the simulation (Figure 4). The A(N7)-G(N2) H-bond of the sheared pair showed modest fluctuation, while the U(N3)-A(N7) H-bond of the rH pair was disrupted after 7 ns (Table 2). The cross-strand A5A14 stack was stable. Conversion of the A5A6 intrastrand stack to an A5G13 stack was clearly seen after 10 ns of simulation (Figure 5).

In the MD_Tt_99 simulation, the major groove width oscillated in the 5-20 Å range (Figure 4B), *i.e.* the original narrow/closed major groove did not convert into a permanently open conformation, in contrast to the previous simulations. The X-ray base-phosphate contact G13(N1)-A5(O2P) (Figure 2) (representing base phosphate interaction type 5BPh) returned as soon as the major groove closed. In addition, new G13(N2)-A5(O2P) H-bond formed, which however fluctuated more than the original X-ray BPh H-bond. Binding mode in which N2 and N1 of G bind to the same anionic oxygen of the phosphate group was recently classified as the alternative of the base phosphate interaction type 4BPh.[1] The simulation thus showed two alternating BPh interaction types. The sheared A/G pair was essentially stable except for a 2 ns disturbance (Table 2) when G13 moved by one base layer and paired with the adjacent A5 base. A long opening event was detected for the U(N3)-A(N7) H-bond of the rH pair (Table 2). Both the cross-strand and intrastrand stacks fluctuated (Figure 5); however, replacement of the intrastrand A5A6 stack by the A5G13 stack was not observed in contrast to previous simulations (see above). At 142 ns, when the major groove closed, the canonical G7=C12 base pair was disrupted. Subsequently, at 152 ns, the adjacent pairs A8-U11 and C9=G10 and the sheared A/G pair broke and the structure was lost. An extension of the simulation to 200 ns did not improve this region, therefore the 150-200 ns time period was not considered in the analysis.

Description of standard MD simulations run with parmbsc0

The 100 ns control simulation of the ribosomal H40 taken from *E.c.* 50S run with parmbsc0 force field[2] (MD_Ec_bsc0, see Table 1) showed picture similar to the corresponding parm99 simulation (MD_Ec_parm99). The simulation revealed opening of the major groove, which, however, was somewhat reduced compared to the MD_Ec_99 simulation (Figure 4B). After ~60 ns, the major groove reached an average width of ~13 Å, around which it oscillated for the remainder of the simulation (Figure 4B). On average, the two measured P-P distances are smaller by ~3 Å compared to the equivalent first 100 ns portion of the MD_Ec_99 simulation. The sheared A/G base pair revealed fluctuation of the A(N7)-G(N2) H-bond. The U(N3)-A(N7) H-bond of the rH base pair showed opening events, and at 65 ns it was disrupted, in a

manner similar to the MD_Ec_99 simulation (Table 2). The intrastrand A5A6 stack and cross-strand A5A14 stack were stable (data not shown).

The control MD_Hm_bsc0 simulation showed widening of the major groove in a manner similar to the MD_Ec_bsc0 simulation, both of which were not as significant as in the parm99 simulation. The parmbsc0 force field contracts the major groove width by ~3 Å on average in the *H.m.* simulation. The major groove width increased to ~14 Å and oscillated around this value (Figure 4B). Opening events were detected for the A(N7)-G(N2) H-bond of the sheared pair and for the U(N3)-A(N7) H-bond of the rH pair (Table 2). The A5 base alternatively stacked with A6 and G13, while the cross-strand stack was stable.

The control MD_Dr_bsc0 simulation showed significant opening of the major groove as in the MD_Dr_99 simulation. After the first 4 ns the major groove width increased to ~15 Å and after 40 ns it reached an average of ~19 Å (Figure 4B). Fluctuation has been seen for the A(N6)-G(N3) H-bond of the sheared A/G pair. The U(N3)-A(N7) H-bond of the rH pair was disrupted after 30 ns (Table 2). In the 0-50 ns time period the A5 base alternatively stacked with A6 and G13, and then stacking established between the A5 and G13 bases in a manner similar to the MD_Dr_99 simulation. The cross-strand stack was stable. For the *D.r.* system, the parmbsc0 and parm99 force fields demonstrated the same average major groove width during the first 100 ns.

In the control MD_Tt_bsc0 simulation, the major groove oscillated in a smaller range from ~8-16 Å (Figure 4B). The systematic difference between the two force fields is ~2 Å. Similar to MD_Tt_99 simulation, the closed major groove was stabilized by the X-ray G13(N1)-A5(O2P) base-phosphate contact and newly formed G13(N2)-A5(O2P) H-bond. Opening events were detected for both non-canonical base pairs (Table 2). The intrastrand and cross-stacks were stable.

The control simulation of the solution structure with parmbsc0 (MD_NMR_bsc0, see Table 1) provided an identical picture as the MD_NMR_99 simulation. In particular, the major groove remained open and the inter-phosphate distances oscillated around the starting values (Figure 4C). The distances were smaller than with the parm99 force field, but only by an average of ~1 Å. The sheared A/G and A/A base pairs were stable. The *c*WS A/U pair was seen in the starting geometry at the beginning and at the end of the simulation, but it assumed the standard *c*WW conformation during the 22-72 ns time period as in the MD_NMR_99 simulation.

LES simulations of ribosomal H40

In the LES_Tt simulation, the internal loop disrupted after the first 3 ns. Subsequently the Watson-Crick segment consisting of residues 7-12 lost its helical geometry and adopted a ladder-like conformation (Figure S8). The structure remained locked in this unsatisfactory arrangement for the rest of the simulation.

In the LES_Hm simulation the internal loop's original base pairing was disrupted after 5 ns and the major groove width increased to 26 Å. At 22 ns the bulging A15 base flipped into the stem for 2 ns to become coplanar with the U4 base. During the rest of the simulation the LES bases formed various arrangements without stable base pairing (data not shown).

Calculation of free energy basin around H40 X-ray structure based on parm99 and parmbsc0 simulations

We have calculated free energy basin around H40 X-ray structure using formula **dG = -kT log (P), where** P(x) refers to probability density.[3] Time periods 0-100 ns of four standard simulations run with force field parm99 and force field parmbsc0 were used (Table 1). RMS deviation from the NMR structure was used as an order parameter. Obtained free energies are shown in Figure S9. The results show that both force fields describe studied system in similar

way and that the free energy barrier for transition between NMR and X-ray structures is higher than 5-6 kcal/mol. It is therefore not surprising that we could not achieve a spontaneous transition. In absence of complete spontaneous transition, we could not better characterize the free energy profile.

Table S1. Simulated annealing protocol used for minimization in the NEB trials.[4]

Step	Steps (2 fs time step)	NEB spring force constant	Procedure Type	Start Temperature (K)	End Temperature (K)
1	1000	10	NVT MD	300	300
2	20000	10	NVT MD with heat up	300	10000
3	100000	50	NVT MD first cooling	1000	500
4	50000	50	NVT MD second cooling	500	300
5	50000	50	NVT MD room temperature	300	300
6	10000	50	NVT MD slow cooling	300	250
7	10000	50	NVT MD slow cooling	300[a]	200
8	10000	50	NVT MD slow cooling	200	150
9	10000	50	NVT MD slow cooling	150	100
10	10000	50	NVT MD slow cooling	100	50
11	50000	50	NVT MD slow cooling	50	0
12	100000	50	Quenched MD	0	0

[a] The initial temperature was mistakenly set to 300 K for this step, where it should have been 250 K. The effect of this error should be negligible on the final result.

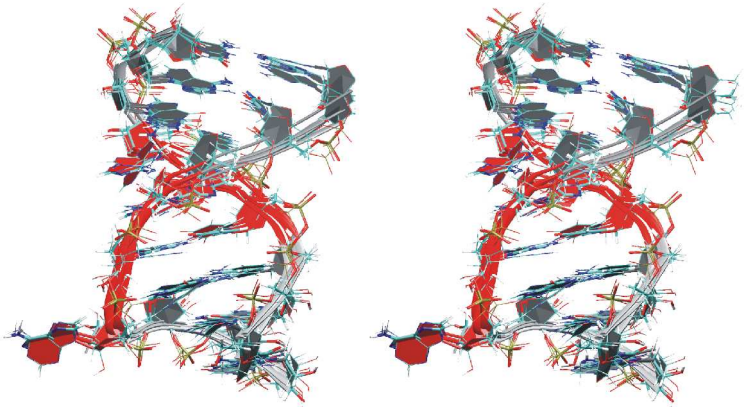

Figure S1. Stereo view of superposition of studied H40 segments from *E.c.*, *H.m.*, *D.r.*, and *T.t.* X-ray structures of 50S subunits. The internal loop is highlighted by red ribbon.

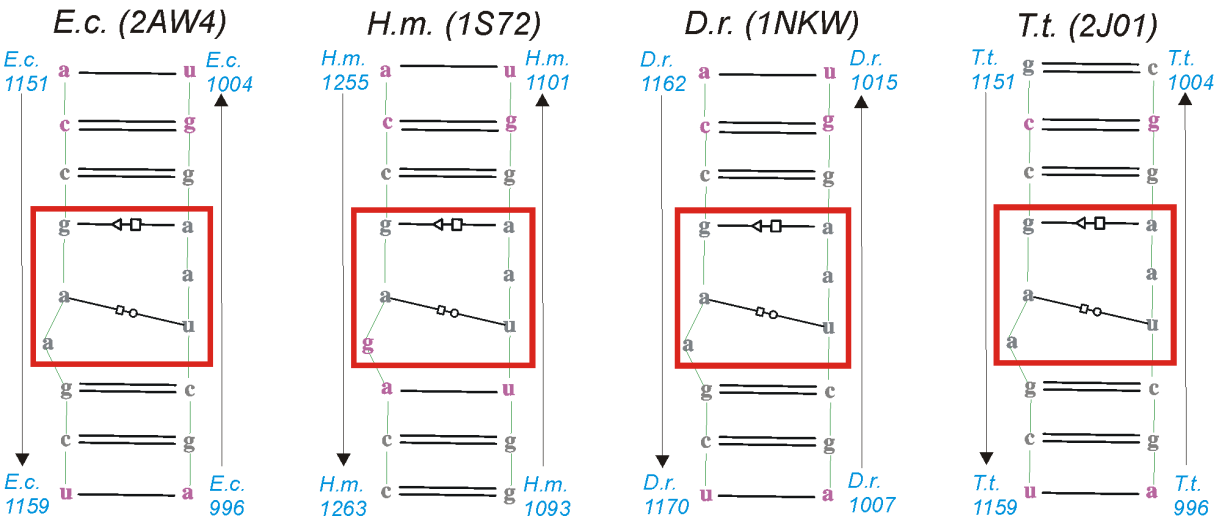

Figure S2. Secondary structures of studied H40 segments with natural X-ray sequences. Original X-ray numbers are in blue. Bases, which were mutated to match the NMR structure (Figure 1C), are in magenta. The internal loop is in the red box.

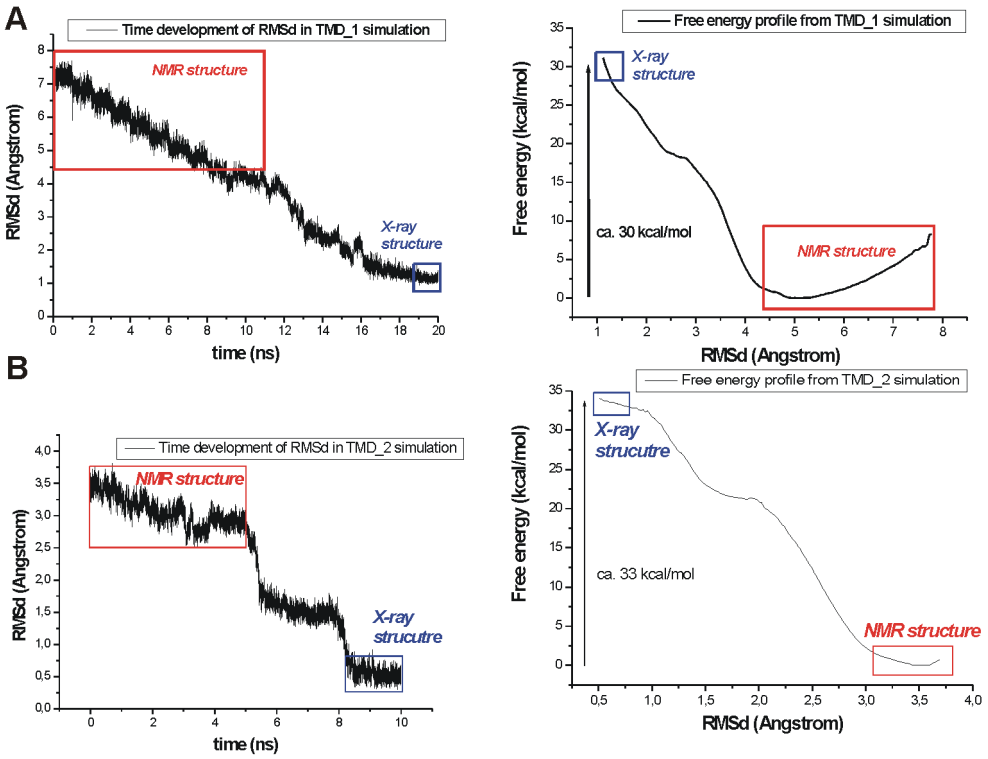

Figure S3. A, B left) RMSd time courses calculated with respect to the X-ray (reference) structure in the MD_TMD_1 and MD_TMD_2 simulations. A, B right) Corresponding free energy profiles. Based on observation of tertiary arrangements adopted in the MD_TMD_1 and MD_TMD_2 simulations the red box indicates the starting NMR conformation while the blue box indicates final X-ray conformation.

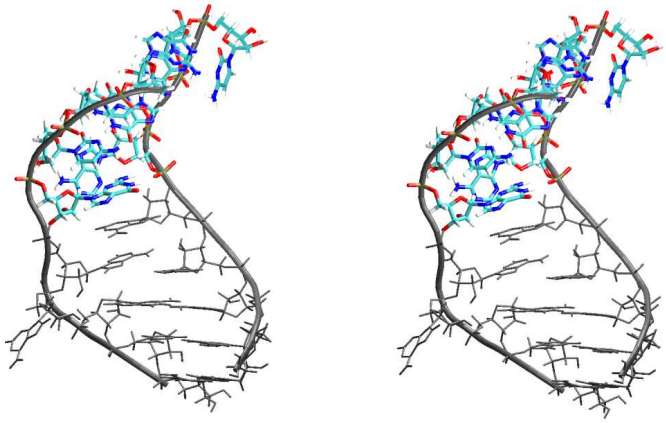

Figure S4. Stereo view of snapshot structure from the MD_Ec_99 simulation at 345 ns. Colored region formed by residues 6-13 is disrupted.

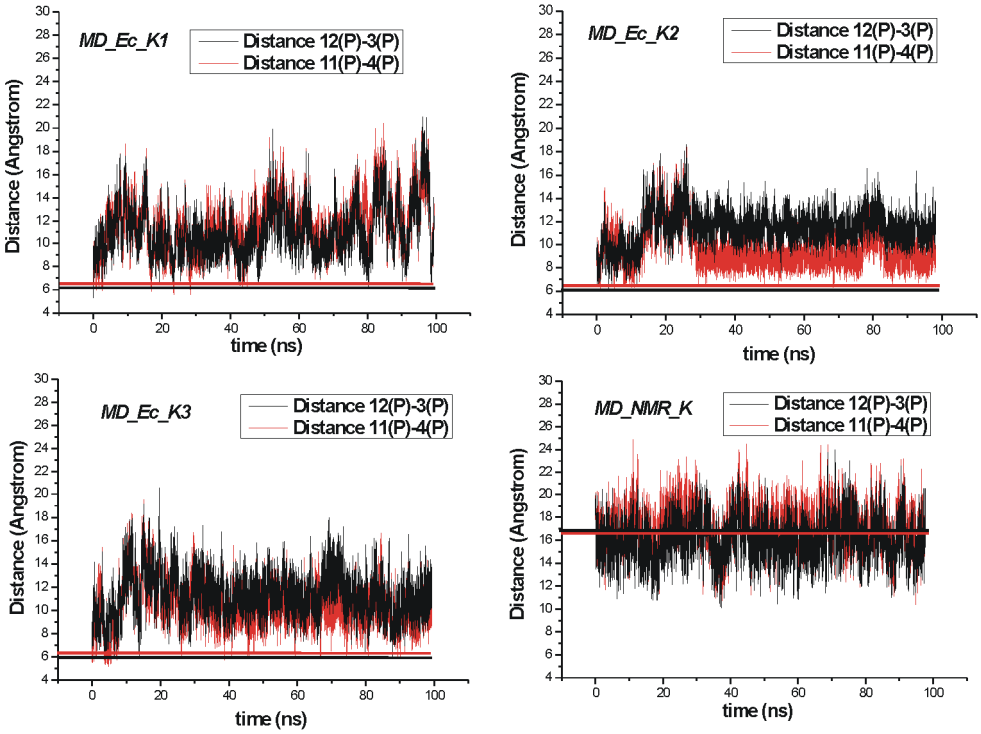

Figure S5. Time course of two inter-phosphate distances across the major groove (11P-4P and 12P-3P) in MD simulations run with excess of KCl ions (see Table 1). Horizontal lines represent the distance in the published structures.

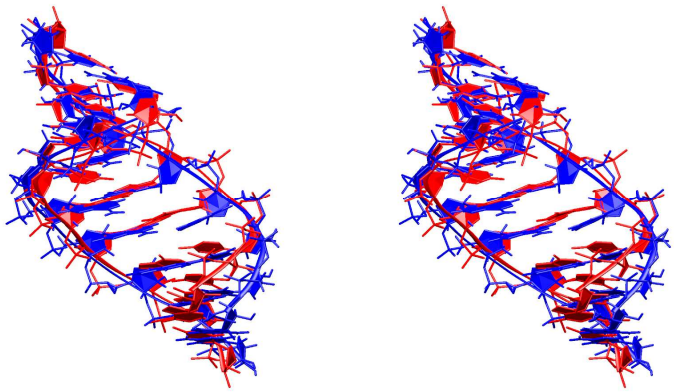

Figure S6. Stereo view of superposition of the NMR solution structure (in red) and the MD structure of H68 (in blue) averaged in the time period 33-100 ns. RMSd between the structures is 1.6 Å.

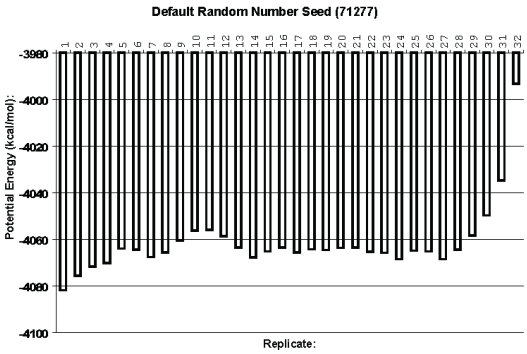
Default Random Number Seed (71277)
Potential Energy (kcal/mol):
-3980
-4000
-4020
-4040
-4060
-4080
-4100
Replicate:

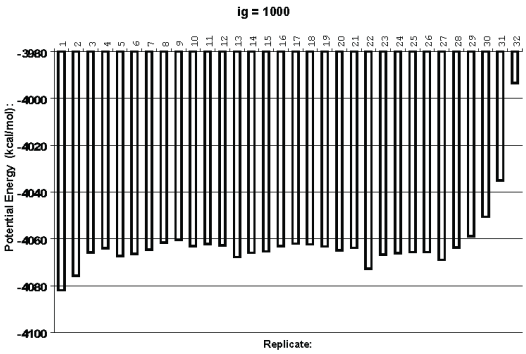
ig = 1000
Potential Energy (kcal/mol):
-3980
-4000
-4020
-4040
-4060
-4080
-4100
Replicate:

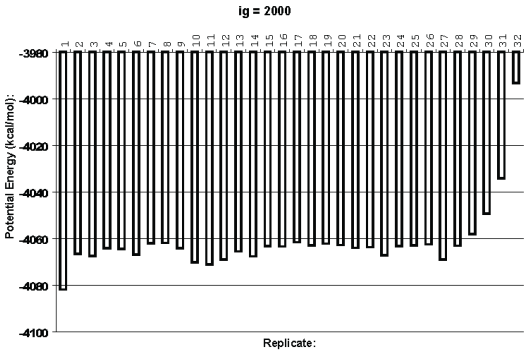
ig = 2000
Potential Energy (kcal/mol):
-3980
-4000
-4020
-4040
-4060
-4080
-4100
Replicate:

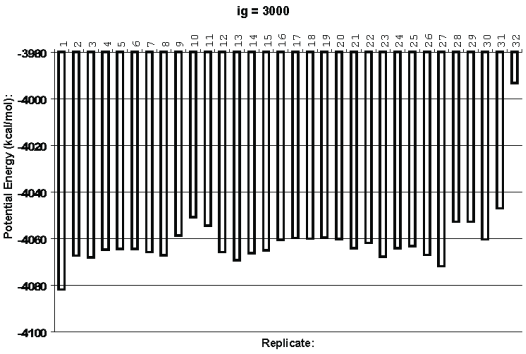
ig = 3000
Potential Energy (kcal/mol):
-3980
-4000
-4020
-4040
-4060
-4080
-4100
Replicate:

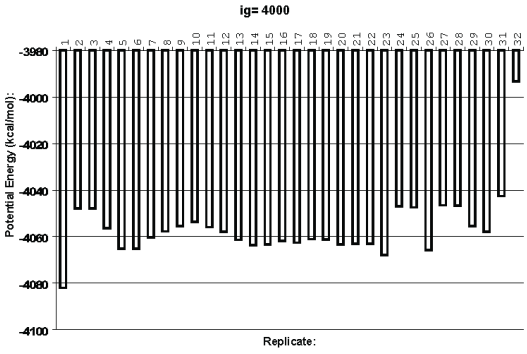
ig= 4000
Potential Energy (kcal/mol):
-3980
-4000
-4020
-4040
-4060
-4080
-4100
Replicate:

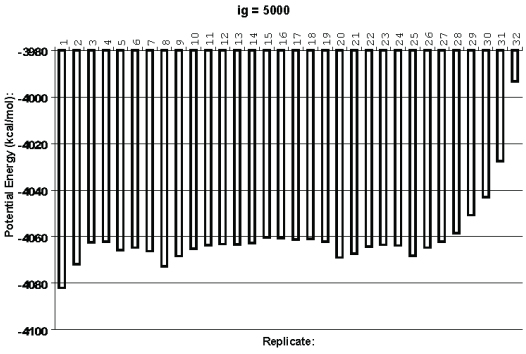
ig = 5000
Potential Energy (kcal/mol):
-3980
-4000
-4020
-4040
-4060
-4080
-4100
Replicate:

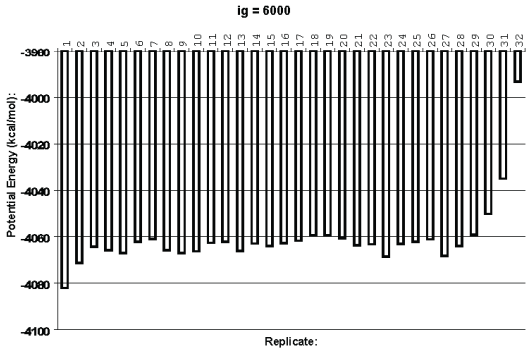
ig = 6000
Potential Energy (kcal/mol):
-3980
-4000
-4020
-4040
-4060
-4080
-4100
Replicate:

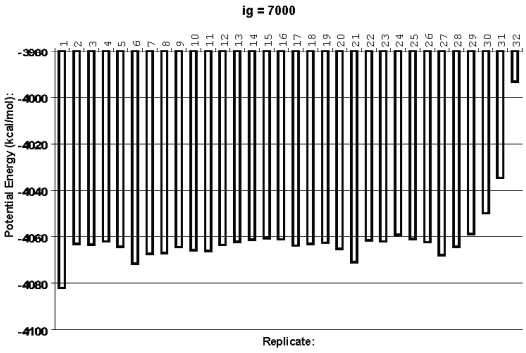
ig = 7000
Potential Energy (kcal/mol):
-3980
-4000
-4020
-4040
-4060
-4080
-4100
Replicate:

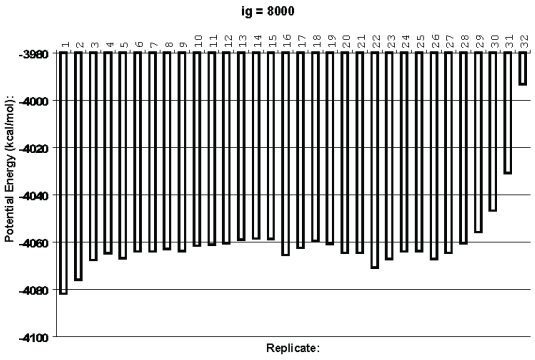
ig = 8000
Potential Energy (kcal/mol):
-3980
-4000
-4020
-4040
-4060
-4080
-4100
Replicate:

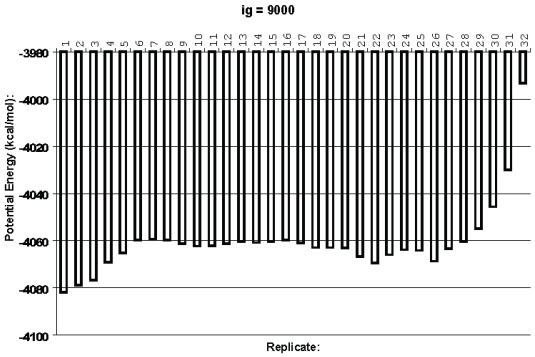
ig = 9000
Potential Energy (kcal/mol):
-3980
-4000
-4020
-4040
-4060
-4080
-4100
Replicate:

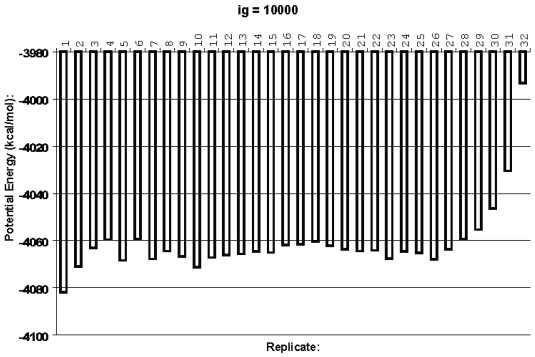
ig = 10000
Potential Energy (kcal/mol):
-3980
-4000
-4020
-4040
-4060
-4080
-4100
Replicate:

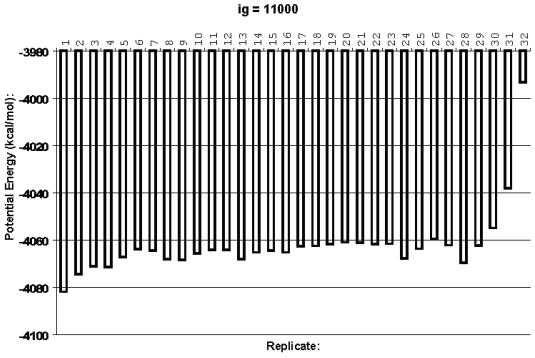
ig = 11000
Potential Energy (kcal/mol):
-3980
-4000
-4020
-4040
-4060
-4080
-4100
Replicate:

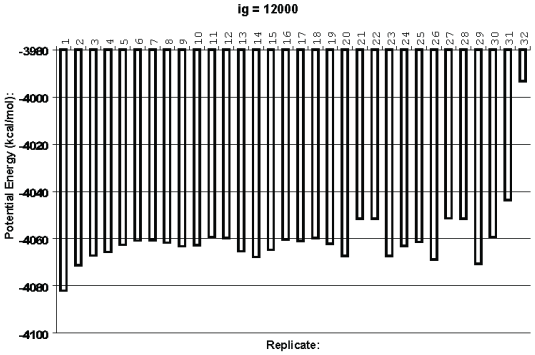
ig = 12000
Potential Energy (kcal/mol):
-3980
-4000
-4020
-4040
-4060
-4080
-4100
Replicate:

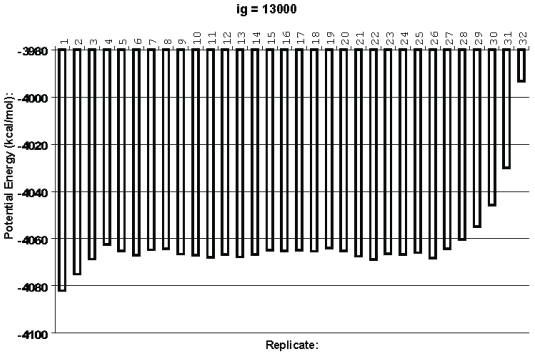
ig = 13000
Potential Energy (kcal/mol):
-3980
-4000
-4020
-4040
-4060
-4080
-4100
Replicate:

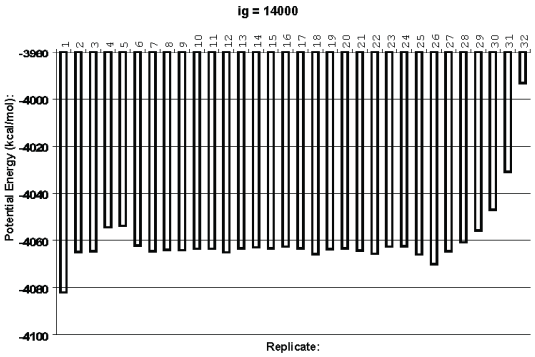
ig = 14000
Potential Energy (kcal/mol):
-3980
-4000
-4020
-4040
-4060
-4080
-4100
Replicate:

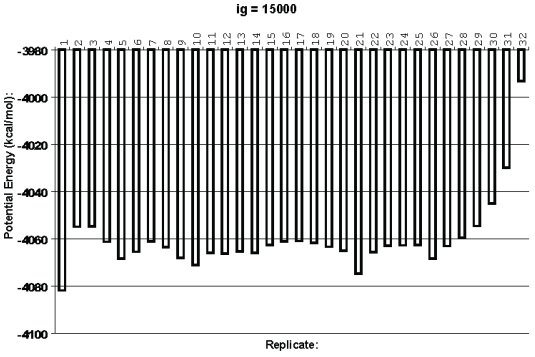
ig = 15000
Potential Energy (kcal/mol):
-3980
-4000
-4020
-4040
-4060
-4080
-4100
Replicate:

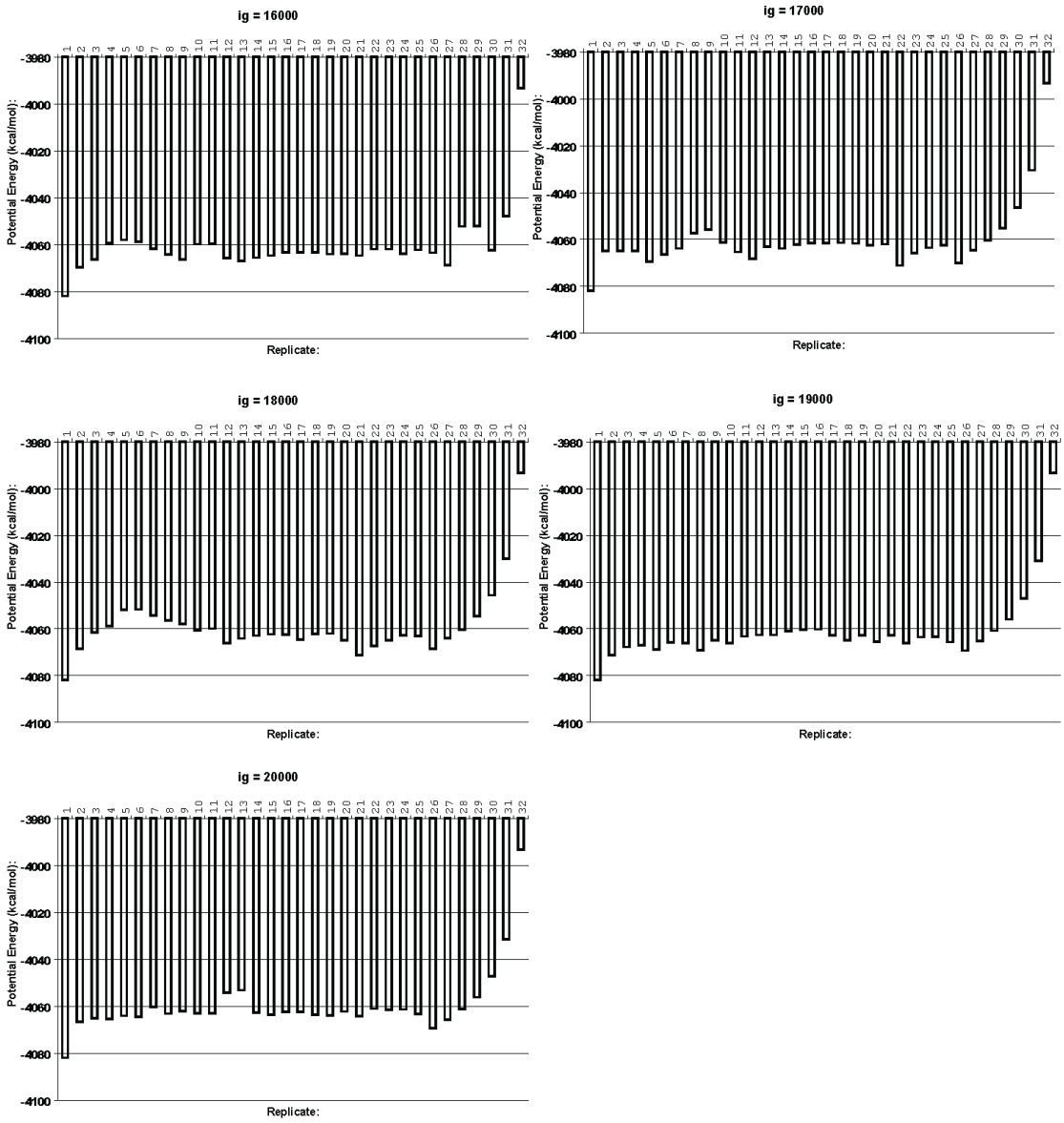

Figure S7. Potential energy plots for 32 image NEB calculations of the internal loop system. Titles indicate the random number seed used. Original is the default random seed of 71277.

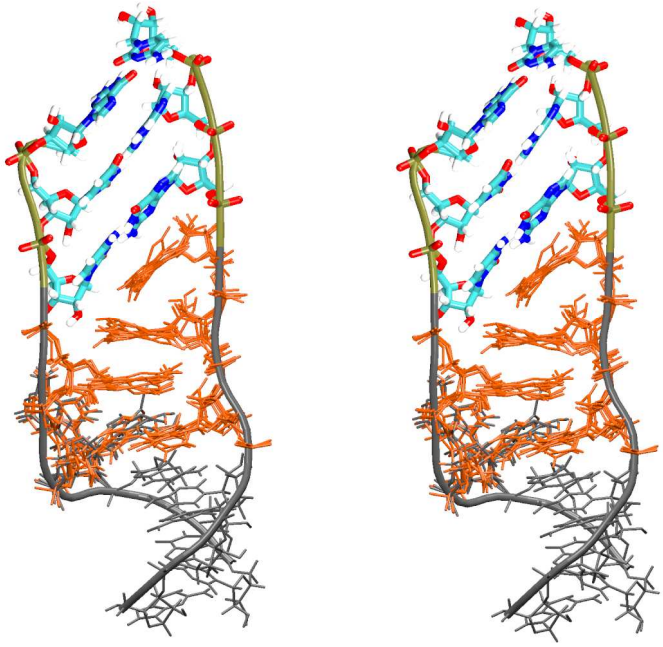

Figure S8. Stereo view of a snapshot structure from the LES_Tt simulation at 36 ns. The canonical segment (colored residues 7-12) lost its helical geometry and adopted a ladder-like conformation. Multiplied bases of the internal loop that are involved in the LES region are in orange.

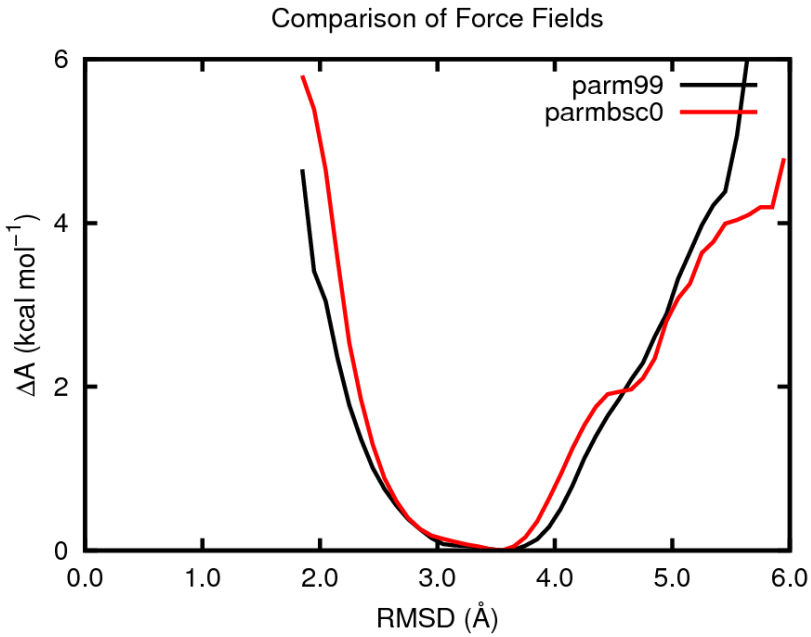

Figure S9. Free energy basin around H40 X-ray structure based on parm99 and parmbsc0 simulations.

Supplemental References

(1) Zirbel, C. L.; Sponer, J. E.; Sponer, J.; Stombaugh, J.; Leontis, N. B. Classification and energetics of the base-phosphate interactions in RNA. *Nucleic Acids Res.* **2009**, *37*, 4898-4918.

(2) Perez, A.; Marchan, I.; Svozil, D.; Sponer, J.; Cheatham, T. E., III; Laughton, C. A.; Orozco, M. Refinement of the amber force field for nucleic acids. Improving the description of α/γ conformers. *Biophys. J.* **2007**, *92*, 3817-3829.

(3) Sanbonmatsu, K. Y.; Joseph, S.; Tung, C. S. Simulating movement of tRNA into the ribosome during decoding. *Proc. Natl. Acad. Sci. U. S. A.* **2005**, *102*, 15854-15859.

(4) Mathews, D. H.; Case, D. A. Nudged elastic band calculation of minimal energy paths for the conformational change of a GG non-canonical pair. *J. Mol. Biol.* **2006**, *357*, 1683-1693.